Available online at www.sciencedirect.com

ScienceDirect

Procedia Engineering 100 (2015) 1092 – 1098

Procedia Engineering

www.elsevier.com/locate/procedia

25th DAAAM International Symposium on Intelligent Manufacturing and Automation, DAAAM 2014

FEM of an Implant Behaviour in a Healthy Bone

Dan Nitoi[a,*], Stefan Milicescu[b], Zoia Apostolescu[a], Andrei Dimitrescu[a], Oana Chivu[a], Marius Cornel Teodorescu[a]

[a] *Dep. of Material Technology and Welding, Univ. Politechnica from Bucharest, Bucharest, Spl. Independentei. No. 313, Romania*
[b] *Dep. of ProsthodonticsFixed, Carol Davila University of Medicine and Pharmacy, Bucharest, Str. Dionisie Lupu no.37, Romania*

Abstract

The human body represents the most important topic for many researchers. In the case of dental medicine, because of the nature of the teeth material, the dimensions and the geometrical position, a very important problem, like fractures, cannot be study with practical classic engineering tools, such as tensometric markers. Under these conditions, the finite element method represents the only method that helps and indicates what is hapening in the structure of maxilar bone and teeth. This paper presents the model and the simulation of the implant under different conditions of mastication forces. In the work, stress and deformation are calculated for different forces acting on the superior zone of the implant. The results are important and gives dental practicians information for the every day work.

Peer-review under responsibility of DAAAM International Vienna

Keywords: implant; bone; FEM; stress; deformation

1. Introduction

Dental implants are designed to provide a foundation for replacement teeth that will look and function like a natural teeth. The implants consist in tiny metal posts which are inserted into the jawbone where teeth are missing. During mastication, important stress are developing as a result of different force that acts on implant surface. Also, important displacement of the implant and jawbone are detected in some loading cases. Because of the geometry, dimensions, and position, the direct measuring of the teeth, implant, bone displacement and stress are very difficult to be measured. Classical methods for measuring the state of stress in a structure involve the use of strain gauges, a situation that can't be possible in analyzing the behaviour of an implant inserted into the bone structure of the mandible or maxilla, components of the human anatomy. Working in this situation is totally different to that of

* Corresponding author. Tel.: +0 074 465 5337 ; fax: +0-000-000-0000 .
E-mail address: nitoidan@yahoo.com

Peer-review under responsibility of DAAAM International Vienna
doi:10.1016/j.proeng.2015.01.471

classical mechanical engineering. Second, the measurement of displacement is also difficult considering the fact that everything is working on human anatomy and classical measurement methods are not applicable. During the research were analyzed many load cases in different situations of bone tender and applying classical techniques of measurement would require a lot of time when that might be applicable. In this situation, analytical calculation methods based on finite element method are the most suitable because they get a very good approximation of the results provided correct input data and achievement of the geometry structure as closely as possible [14],[17]. Consequently, we chose this research method [12] because experimental methods do not give satisfactory results when analyzing human structures. This method enabled the successful determination of movements and stress in the bone and implant, as they are the most important data used by dentists. They need customization works because each person is unique and implants behaviour is not similar in any situation. The displacements and strains prognosis is important to achieve the shape and size of blunt attachment and crown. The FEM can be used with success in the condition of very good approximation of all the data [1],[4], [13].

Paper presents the modelling and simulation of an inserted implant into the jawbone structure that consists in cortical and trabecular bone [11]. The analysis was performed to predict the system bone-implant behaviour in different loading conditions and bone resorption. The study presents the case of a healthy jawbone followed by different bone resorption values.

The jawbone consists in a trabecular zone placed below the cortical bone which fixes the implant. Two forces are acting on the implant on vertical and horizontal directions with different values presented in table 1 [2], [3],[7], [8], [9],[16]. Figure 1 presents the studied structure that consists in the cortical bone, trabecular bone, implant and abutment. The implant with the diameter $\theta = 3.75$ mm and length $l = 11$ mm is inserted into the cortical bone.

Table 1. Loading case of an implant.

Case/force	F_x [N]	F_z [N]
a	100	-75
b	125	-75
c	150	-75
d	100	-100
e	125	-100
f	150	-100

In the implant superior part it is placed the abutment as it is presented also in figure 1a [10]. The model is designed according to mechanical and physical properties of materials [5].

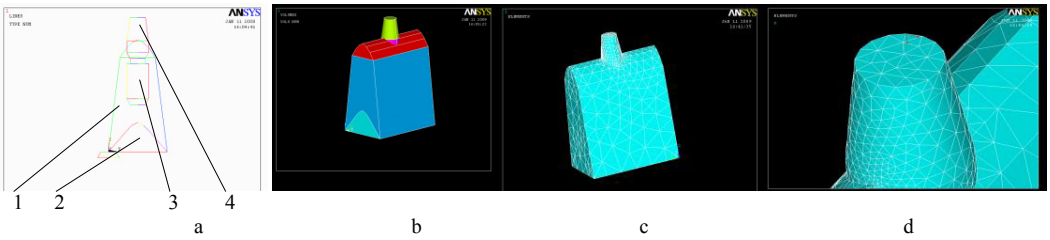

Fig.1. FEM input data; (a) Structure geometry 1 – cortical bone; 2 – trabecular bone; 3 – implant; 4 - abutment; (b) bone-implant-abutment structure; (c) spatially discretized structure; (d) application of the loading forces.

Figure 1b presents a spatial image of the assembly bone-implant-abutment. To solve the problem, the structure has to be spatial discretised as it is presented in figure 1c. The loading system consists of two forces that act on the abutment frontal face. The loading values are presented in table 1, direction and force direction are presented in figure 1d. In the first study, the applied forces are Fx = 100 N and Fz= -75 N, and the structure is deformed and important stress appears.

2. Stress And Displacement Calculation For The Bone-Implant - Abutment System

As a result of applied forces, on the OX axis, displacement developed are presented in the figure 2a, and b. From the image analysis, the important zones like bone and abutment are studied. From this viewpoint, the displacement of the cortical bone is about $UX_{bone} = 0.45 \cdot 10^{-4}$ m. The abutment moves at the point $UX_{abut} = 0.83 \cdot 10^{-4}$ m, but both values are not important at this point.

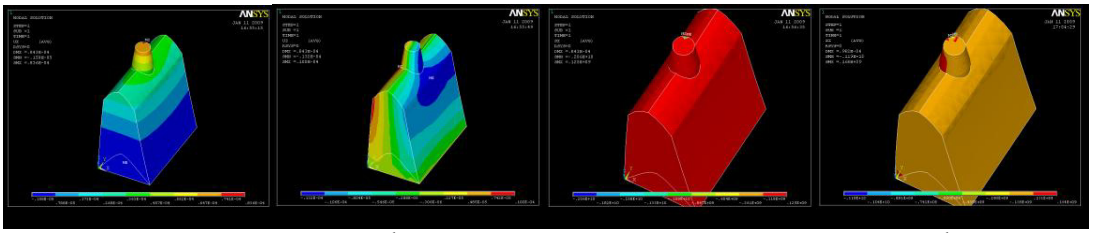

a b c d

Fig. 2. Structure deformation and stress on the first loading case; (a) OX axis deformation, (b) OZ axis deformation, (c) OX axis stress, (d) OZ axis stress.

The structure displacement on the OZ axis is showed in figure 2b where the bone and abutment has the same maximal displacement $UZ_{abutment} = UZ_{bone}$ $0.13 \cdot 10^{-4}$ m. From the point of view of the calculated stress, figure 2c presents the OX stress. The maximal stress values refer to the bone structure. Because the implant material is Titanium low stress values is developed. The bone stress has to be studied and the maximal value on the OX axis is $SX = 0.12 \cdot 10^{9}$ N/m^2. The value, in this loading case, is not great in proportion with cortical bone Young modulus but very close to trabecular bone elasticity modulus. From this point of view the loading case is very near to permanent deformations of this bone type with possible repercussion in the mastication process [6]. On the OZ axis, maximal stress has the value $SZ = 0.13 \cdot 10^{8}$ N/m^2 for the both kind of bones but the value is not important and the structure has elastic behaviour.

The second loading case consists in the Fz = -75 N and Fx = 125 N forces. The maximal displacement on the OX axis are $UX_{bone} = 0.87 \cdot 10^{-4}$ m. and $UX_{abut} = 0.98 \cdot 10^{-4}$ m. These values are greater than in the first case but are also with no importance in the mastication process and are presented in figure 3a. For the OZ axis, the corresponding image is 3b and the deformations are $UZ_{bone} = UZ_{abut} = 0.15 \cdot 10^{-4}$ m. The values are higher than in the first case but also with no functional implications.

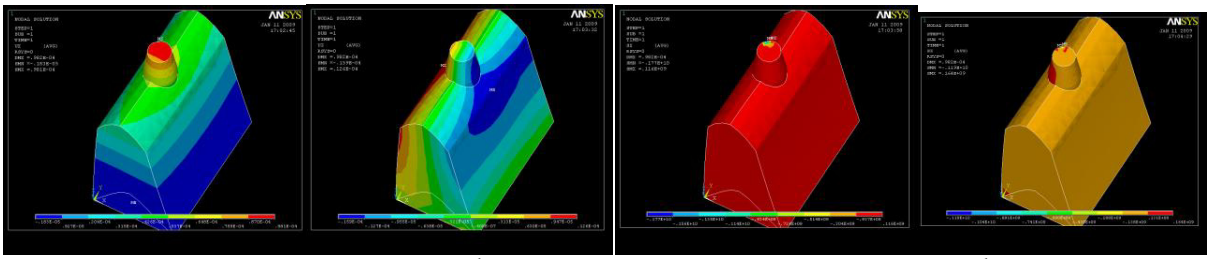

a b c d

Fig. 3. Structure deformation and stress on the second loading case; (a) OX axis displacement; (b) OZ axis displacement; (c) OX axis stress; (d) OZ axis stress.

Stress on the OX axis (fig. 3.c), $SX_{bone} = 0.116 \cdot 10^{9}$ N/m^2, is near the same with the first loading case and implies an elastic behaviour. Bone stress that refers to OZ axis (fig. 3d) is also the same with the first case, $SZ = 0.13 \cdot 10^{8}$ N/m^2. On the inferior part of the bone, stress values are greater and near the elasticity modulus of the spongious bone, $SZ = 0.16 \cdot 10^{9}$ N/m^2. A close analysis of the image shows high stress values in the cortical bone, but very close to spongious bone.

The third loading case consists in mastication force values Fx = 150 N şi Fz = -75 N. In this situation, the OX deformation values (fig.4a) are $UX_{bone} = 0.1 \cdot 10^{-3}$m and $UX_{abut} = 0.12 \cdot 10^{-3}$ m, are important, in the field of tenth of

millimetre. For the OZ axis, the corresponding displacement values are presented in figure 4b and the maximal values are about UZ = $0.19 \cdot 10^{-4}$ m. These values are about hundredth of millimetre and don't present any problems from this point of view.

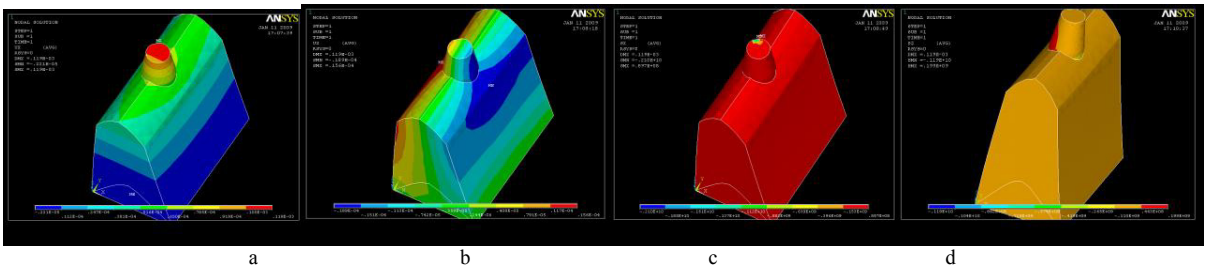

a b c d

Fig. 4. Structure deformation and stress on the third loading case; (a) OX axis displacement; (b) OZ axis discplacement; (c) OX axis stress; (d) OZ axis stress.

In figure 4, the stress map presents the OX and OZ values. On the first situation (fig.4c), the maximal value is SX = $0.15 \cdot 10^{9}$ N/m^2, value not important for the cortical bone but near the Young modulus of the trabecular bone. A higher OZ stress maximal value is SZ = $0.26 \cdot 10^{9}$ N/m^2, presented in figure 4d.

The fourth loading case considers an increased force Fx = 100N and smaller value for Fz = -100 N. On the OX axis, the maximal displacement value is $UX_{bone} = 0.49 \cdot 10^{-4}$ m and $UX_{abut} = 0.75 \cdot 10^{-4}$ m. and is presented in figure 5a. Image 5b presents the displacement on the OZ axis with the maximal value UZ= $0.13 \cdot 10^{-4}$ m.

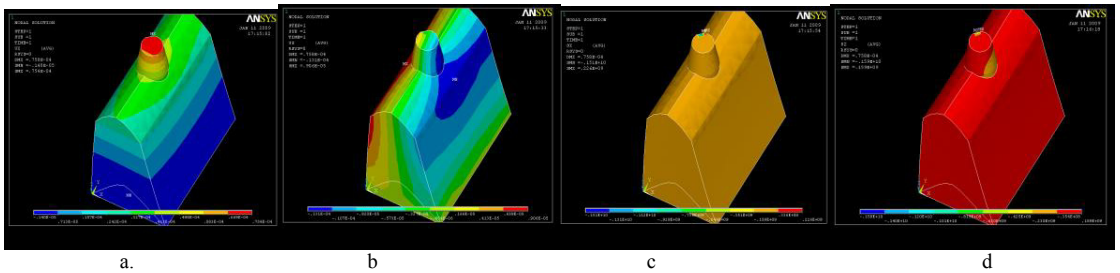

a. b c d

Fig. 5. Structure deformation and stress on the fourth loading case, (a) OX axis displacement; (b) OZ axis displacement; (c) OX axis stress; (d) - OZ axis stress.

For the fourth loading case, figure 5c presents the stress on the OX axis with the maximal value SX = $0.15 \cdot 10^{10}$ N/m^2. The OZ axis stress (fig. 5d) has the maximal value SZ = $0.16 \cdot 10^{9}$ N/m^2, below the Young Modulus of the cortical and spongious bone. Thus, the system behaviour is elastic.

The fifth loading case consists in the force action Fz = -100 N and Fx = 125 N. For this situation, the maximal structure displacement on the OX axis are $UX_{bone} = 0.13 \cdot 10^{-3}$ m and $UX_{abut} = 0.2 \cdot 10^{-3}$ m. These values are important and cannot be negligible (fig.6a). For the OZ axis, in figure 6b, the maximal bone and abutment displacement, UZ = $0.36 \cdot 10^{-4}$ m, are quite equal and not important.

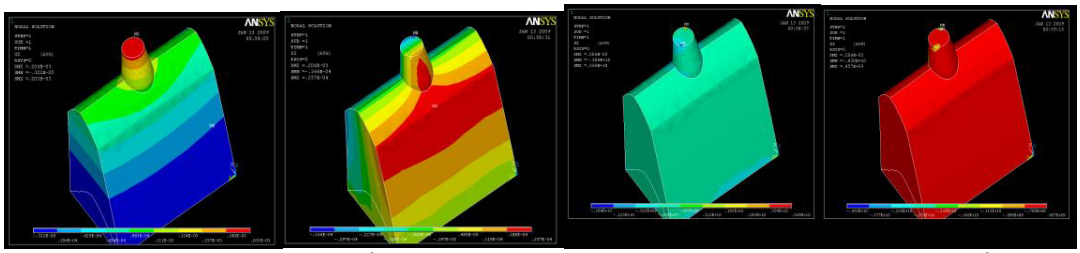

a b c d

Fig. 6. Structure deformation and stress on the fifth loading case; (a) OX axis; (b) OZ axis; (c) - OX axis stress; (d) - OZ axis stress.

The stress on the OZ axis is presented in figure 6d with the maximal value SZ = $0.45 \cdot 10^9$ N/m^2. Figure 6c depicts the OX stress axis with the difference of the cortical and trabecular bone. On the trabecular bone, while the maximal stress is $SX_{sp} = 0.12 \cdot 10^{10}$ N/m^2, the maximal stress on the cortical bone being $SX_{cor} = 0.6 \cdot 10^9$ N/m^2. Starting with this loading case, the stress refers to dangerous values especially for the trabecular bone which can suffers plastic deformations.

In the sixth loading case, when the forces values are greater, the OX maximal displacement for the bone is $UX_{bone} = 0.74 \cdot 10^{-4}$ m and for the abutment $UX_{abut} = 0.9 \cdot 10^{-4}$ m (fig.7a). The presentation for the OZ displacement is done in figure 7b that shows a maximal value UZ = $0.16 \cdot 10^{-4}$ m.

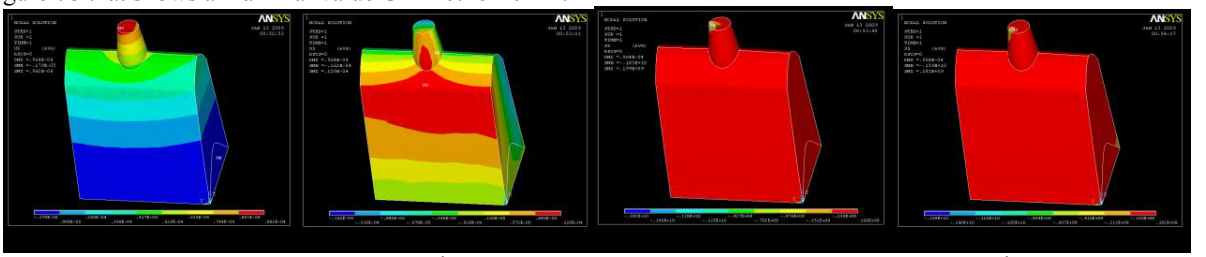

a b c d

Fig. 7. Structure deformation and stress on the sixth loading case; (a) OX axis displacement; (b) OZ axis displacement; (c) OX axis stress; (d) - OZ axis stress

Figure 7d presents the stress that acts on the OZ axis with the maximal value in the bone $SZ_{bone} = 0.18 \cdot 10^9$ N/m^2. This value is lower than the Young modulus of the both bone type. For the OX axis, the stress map indicates a maximal value SX = $0.19 \cdot 10^9$ N/m^2 (fig. 7c).

3. Conclusions

The finite element method represents a very useful tool used in engineering design. The medical discipline became a relatively new branch that derives benefits from this powerful calculation software. For a better understanding, in the following paragraphs, the graph variation of the stress and displacement that resulted in the bone-implant-abutment will be presented. One of the problems to be solved by practicing medical doctors is the knowledge of implant displacement through tenses. These displacements that may cause crown friction during chewing or cracks in situations where contact between them is strong, caused by large displacements, resulting from the applied tenses field or bone tender, not always optimal. Another important element, shown in Figure 8, is the analysis of bone deformations, strains that can cause even its crack. For this type of response (bone deformities), FEM is the most simple, safe and accurate calculation method.

Figure 8 presents the bone and abutment deformations on the OX and OZ axis in the first three loading cases, at a constant Fz = 75 N force. These values are increasing and the remark refers to the same bone and abutment displacement on the OX and OZ axis. Calculated maximum values are tenths of mm, values which, if compared to tooth structure, are very important.

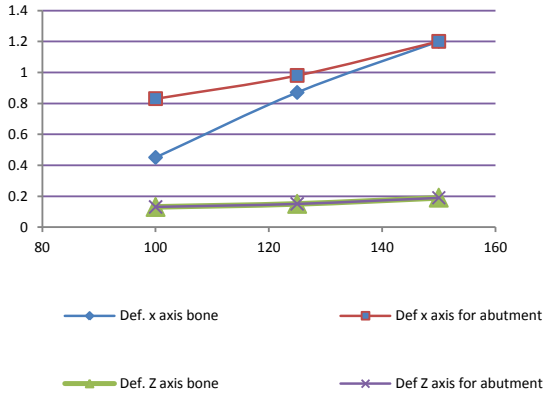

Fig. 8. Bone and abutment deformations on the OX and OZ axis in the first three loading cases, at Fz = 75 N.

The second important set of results concerns the stress analysis. The stress to be interpreted refers to those developed in the bone structure because they can cause fractures and are those that can cause pain during mastication. Implant mechanical stress, don't have high values compared to the elasticity modulus of the material and the subject of the article is the study from human point of view, anatomic, not mechanically realization of the implant.For the first three loading cases, figure 9 presents the bone stress on the OX and OZ axis. This variation is important because the abutment induced stress is not high and oral health can be influenced by a high bone stress. In the third loading case, the bone starts to have important stress, very near to the elasticity modulus that may imply potential damages [2].

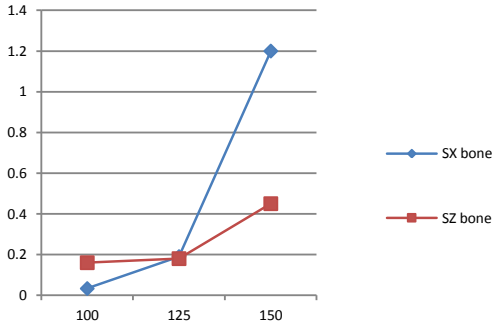

Fig. 9. Bone displacement on the OX and OZ axis.

Figure 10, presents the last three cases of bone and abutment displacement, at the acting force Fz = 100 N. As it is normal, most important bone deformations are on the OX axis which reaches very important level for the last loading case. As it is normal, these deformations have higher values than the previous case with deformations leading to tenths of a millimeter. The calculated values may cause displacement of the implant crowns, the contact between them and possible cracking. Calculated values, as shown in Figure 10, the bone at the end UXbone = 0.15 mm, an important value taking into account the distances between crowns that are often smaller than these values.

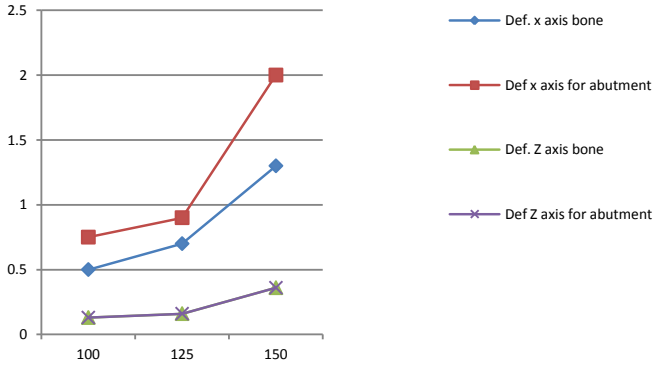

Fig.10. Bone and abutment deformations on the OX and OZ axis in the last three loading cases, at Fz = 100 N.

The FEM resolves an important problem of practical dental medicine when the knowledge about the forces that can be supported by an implant is crucial in long time duration of the dental work. Being prepared with theoretical information about each teeth structure, the dental doctors are more informed and better prepared for each surgical activity. By modelling, each geometric and functional particularity can be better understand and the implant rate of success is increased.

For an even better modelling and simulation of implants behaviour in different cases of bone resorption and different loading situations, still aims to implement a much better geometric model, based on the implant area scan of each patient. The image thus obtained can then be inserted into the finite element programs and afterwards analyzed according to the specific application conditions of the patient.

4. References

1. D. Nitoi, Gh. Amza, Modeling and simulation of technological processes, Agir Publishing House, 2009.
2. Ou KL, Chang CC, Chang WJ, Lin CT, Chang KJ, Huang HM. Effect of damping properties on fracture resistance of root filled premolar teeth: a dynamic finite element analysis. *Int. Endod J* 2009;42:694-704.
3. A. Geramy, Apical third morphology and intrusive force application: 3D finite element analysis. J Dent Tehran Univ Med Sci 2007,4(3):130-134.
4. I. Lock, M. Jerov, S. Scovith, (2003) Future of modeling and simulation, IFMBE Proc. vol. 4, World Congress on Med. Phys. & Biomed. Eng., Sydney, Australia, 2003, pp 789–792.
5. V. Lertchirakarn, JEA. Palamara, HH. Messer, Anisotropy of tensile strength of root dentine. *J Dent Res* 2001;80:453-456.
6. D. Niţoi, C. Amza, M. Iliescu, FEM stress analisys for molar teeth, pag 238, Recent Advances in information Science Proceeding of the 4-th European Conference of Computer Science (ECCS), Paris, october, 29-31, 2013.
7. B. Akkayan, T. Gulmez, Resistance to fracture of edodontically treated teeth restored with different post systems, Journal of Prosthetic Dentistry 87, 2002, 431-437.
8. P. Ausiello, AL. DeGee, S. Rengo, CL. Davidson, Fracture resistance of endodontically-treated premolars adhesively restored, Am J Dent 10, 1997,237-243.
9. C. Canalda-Sahli, E. Brau-Aguadé, E. Berástegui-Jimeno, A comparison of bending and torsional properties of K-files manufactured with different metallic alloys, Int Endod J 29, 1996, 185-195.
10. HG. Cooke, FL. Cox, C-shaped canal configurations in mandibular molars, Journal of American Dental Association 99, 1982, 836-839.
11. AA. Iliescu, CM. Petcu, D. Niţoi, A. Iliescu, Chewing Stress Developed in Upper Anterior Teeth with Root end Resection. A Finite Element Analysis Study, Chirurgia, Vol. 108, 2013, 389-395.
12. A. Sivitski, P. Podra, Finite element method and its usable applications in wear models design, 9th International DAAAM Baltic Conference, Industrial Engineering, 24-26 April 2014, Tallinn, Estonia.
13. A. Celaya, I. Etxeberria, O. Gonzalo, L.N. Lopez de Lacalle, An experimental approach for the assesment of a FEM model of ortogonal cutting, The 13th International DAAAM Simposium, Intelligent manufacturing & automation Learning from Nature, 23-26 Octomber, 2002.
14. SD. Mohammed, H. Desai, Basic Concepts of Finite Element Analysis and its Applications in Dentistry: An Overview. Oral Hyg Health 2:156. doi: 10.4172/2332-0702.1000156, 2014
15. Lamvohee JMS, Ingle P, Cheah K, Dowell J and Mootanah R, (2014) Total Hip Replacement: Tensile Stress in Bone Cement is influenced by Cement Mantle Thickness, Acetabular Size, Bone Quality, and Body Mass Index. J Comput Sci Syst Biol 2014, 7: 072-078 doi: 10.4172/jcsb.1000140
16. Lamvohee JMS, Ingle P, Cheah K, Dowell J and Mootanah R, (2014) Total Hip Replacement: Tensile Stress in Bone Cement is influenced by Cement Mantle Thickness, Acetabular Size, Bone Quality, and Body Mass Index. J Comput Sci Syst Biol 2014, 7: 072-078 doi: 10.4172/jcsb.1000140
17. Walker RW, Cheah K, Ingle P and Mootanah R, (2013) Stress in the Patella Following Autologous Chondrocyte Implantation - A Finite Element Study. J Comput Sci Syst Biol 2013, 6: 305-310 doi: 10.4172/0974-7230.1000126